narrowing of the effective cross section available for flow because of the presence of the body. This causes a decrease in boundary-layer thickness at the wall. In addition, the fluid obtains, owing to the deflection by the body, a velocity component perpendicular to the tube wall that also decreases the boundary-layer thickness. The first effect is most intense at $x \approx 0$ and the second at $x \approx -R$. Owing to the superposition of the two effects, the first maximum for the Sh number occurs for $-R < x < 0$. Exceptions are the curves for the disk, because in this case the deflection occurs only at $x \approx 0$. Consequently, the first maximum is immediately behind the point $x = 0$.

The minimum and second maximum for the curves are due to the annular wake, formed behind the body, and its effect on the fluid flow. Fluid behind the body is sucked into the wake, causing an increase of boundary-layer thickness at the wall. This leads to the decrease of the local Sherwood number.

Owing to the instability and separation of the wake beyond the body, the turbulence intensity increases in the zone beyond the wake. The turbulent pulsations penetrate deeper into the laminar sublayer, causing a reduction of the diffusion sublayer thickness. This leads to the increase of the local Sherwood number.

For bodies of identical diameters, the difference between the minimum and second maximum is the smallest for the sphere, larger for a hemisphere, and the largest for a disk, because the wake beyond the bodies of these geometries gains intensity in the same order. This also applies to the values of the Sherwood number at the second maximum. The difference in the Sh number between the minimum and second maximum, as well as the value at the second maximum, increases with increasing Reynolds number for the same reasons.

The analysis of the results for spheres of different diameters indicates an increase in the Sh number at both maxima and an increase of the difference between the minimum and second maximum with the increase of sphere diameter. This is due to the decrease of the free cross section between the sphere and the wall, as well as between the wake and tube wall, resulting in a higher influence of the sphere and wake beyond it on the velocity gradients along the walls.

NOTATION

c_o = bulk methylene blue concentration in the fluid
C_p = surface concentration of methylene blue on the silica gel transferred during stationary flow
d = tube diameter
D = diffusion coefficient
k = mass transfer coefficient
R = body radius
Re = Reynolds number
Sh = local Sherwood number
x = distance along the tube
θ = stationary adsorption time

LITERATURE CITED

Cvijović, S. D., and M. V. Mitrović, "Presentation and Verification of One Modification of the Adsorption Method for Mass Flux Measuring," *Bull. Soc. chim. Beograd*, **34**, 453 (1969).

Duduković, A. P., Graduation Work, Faculty of Technology and Metallurgy, Beograd (1974).

Končar-Djurdjević, S. K., "Adsorption Under Fixed Hydrodinamic Conditions," *Bull. Soc. chim. Beograd*, **14**, 233 (1949).

———, "Application of a New Adsorption Method in the Study of Flow of Fluids," *Nature*, **172**, 858 (1953).

———, "Eine neue allgemeine Methode zur Untersuchung der Wirkungsweise chemischer Apparaturen," *Dechema-Monographien*, **26**, 139 (1956).

———, and A. P. Dudukovic, "The Influence of Bodies Placed in the Fluid Stream on the Mass Transfer Rates to the Tube Walls," presented at CHISA, Prague (1975).

Mitrović, M. V., Dissertation, Faculty of Technology and Metallurgy, Beograd (1965).

———, and S. K. Končar-Djurdjević, "Adsorptionsuntersuchung einer losung auf rotierenden scheiben," *Bull. Soc. chim. Beograd*, **28**, 393 (1963).

Popović, G. and S. K. Končar-Djurdjević, "Messung der Lokalen Koeffizienten des Massenubergangs auf Zylindrische Oberflachen unter Bestimmten Hydrodynamischen Bedingungen," *ibid.*, 242 (1963).

Vukovic, O. B., and S. K. Končar-Djurdjević, "The analogy Between a Convective Mass Transfer and the Momentum," *ibid.*, **40**, 455 (1975).

Manuscript received April 23, 1976; revision received July 15 and accepted July 22, 1976.

Prediction of Heat Transfer Coefficients in Drag Reducing Turbulent Pipe Flows

AFSHIN J. GHAJAR and WILLIAM G. TIEDERMAN

Oklahoma State University
Stillwater, Oklahoma 74074

In this prediction method, an eddy diffusivity model proposed by Cess (1958) and the Reynolds analogy are used to integrate the momentum and energy equations for the case of constant heat flux in fully developed, turbulent pipe flows. The unique feature is that in drag reducing flows, it is not possible to determine one of the constants in the eddy diffusivity model a priori. An iterative scheme proposed by Tiederman and Reischman (1976) is used to determine the constant A^+ which characterizes the thickness of the near-wall region of the flow. This iterative scheme requires as inputs an experimental value for the von Karman constant K and some initial guess for A^+. The procedure then determines an exact value for A^+ and integrates the equations to yield velocity and temperature profiles. From this point, heat transfer calculations are straightforward, as the heat transfer coefficient is then determined by evaluating the temperature gradient at the wall and the mixed mean or bulk temperature of the flow.

ANALYSIS

The eddy diffusivity expression proposed by Cess (1958) is

$$E = \frac{\epsilon_M}{\nu} = \frac{1}{2}\left\{1 + \frac{K^2 r_o{}^{+2}}{9}[1 - (r/r_o)^2]^2\right.$$

tube diam from the entrance so that the flow in the tube was fully developed prior to reaching the obstruction. The spheres were fixed by a steel shaft, 1.8 mm thick, mounted perpendicular to the flow direction. Other bodies had an additional support for maintaining the desired position. It was found that the supporting shafts interfered with the flow only slightly and affected the adsorption spectrum only within several millimeters of the shafts.

The diameters of the spheres were 30, 40, and 50 mm and of the hemisphere and disk 40 mm. The hemisphere was mounted so that the spherical part faced the upstream direction. The 3 mm thick disk, tapered around the circumference at a 45 deg. angle in the downstream direction, produced an effect analogous to that of an extremely thin disk placed in the fluid stream.

Silica gel coated foils were placed on the tube wall around the body. Owing to their flexibility, the foils fully adhered to the tube wall.

RESULTS

Experiments were made of local mass transfer as a function of the distance along the tube at different Reynolds numbers, and for the sphere, a dependence on the ratio of sphere and tube diameters was also investigated.

The total adsorption time was 6 min; 1 min was required for filling and emptying the operating tube and 5 minutes for adsorption at stationary flow conditions. Independent measurements were made of the mass transferred per unit surface area during tube charge and discharge. This was subtracted from the total mass transferred per unit surface area during the experiment, yielding the mass transferred per unit area during stationary flowing under desired conditions.

When the conditions under which mass transfer by adsorption may be considered stationary are satisfied, the coefficient of mass transfer may be determined. Since the methylene blue concentration in the fluid immediately above silica gel surface, as demonstrated, may be considered in our case as approximately equal to zero, a simplified equation is obtained:

$$k = \frac{C_p}{\theta \cdot c_o}$$

Local Sherwood numbers were calculated as

$$Sh = \frac{k \cdot d}{D}$$

and are presented as a function of the distance along the tube, where $x = 0$ is the normal projection of the body center on the tube wall. The positive direction of the x axis is in the direction of fluid flow. Individual curves in Figures 1 to 5 correspond to different values of Reynolds numbers.

Figures 1, 2, and 3 show the effects of the 30, 40, and 50 mm spheres on the local mass transfer along tube wall for different ratios of sphere and tube diameters (1/2, 2/3, 5/6).

Figure 4 shows the effect of the 40 mm diameter hemisphere on local mass transfer and Figure 5 the effect of the 40 mm diameter disk.

DISCUSSION

The curves in Figures 1 through 5 which show the dependence of the local Sherwood number on the distance along the tube have several common characteristics for all bodies and all Reynolds numbers. At larger distances in front of and behind the body, all curves tend to reach some

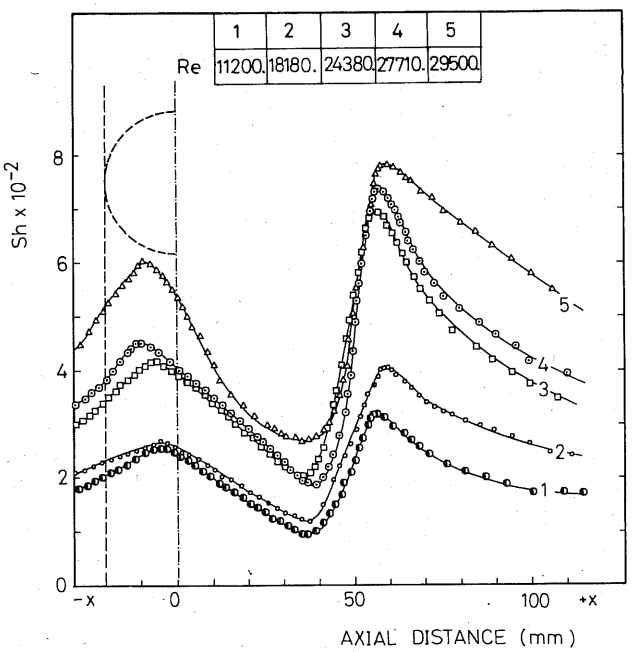

Fig. 4. Local Sherwood number vs. tube wall length. Coaxially hemisphere of 2/3 *d*.

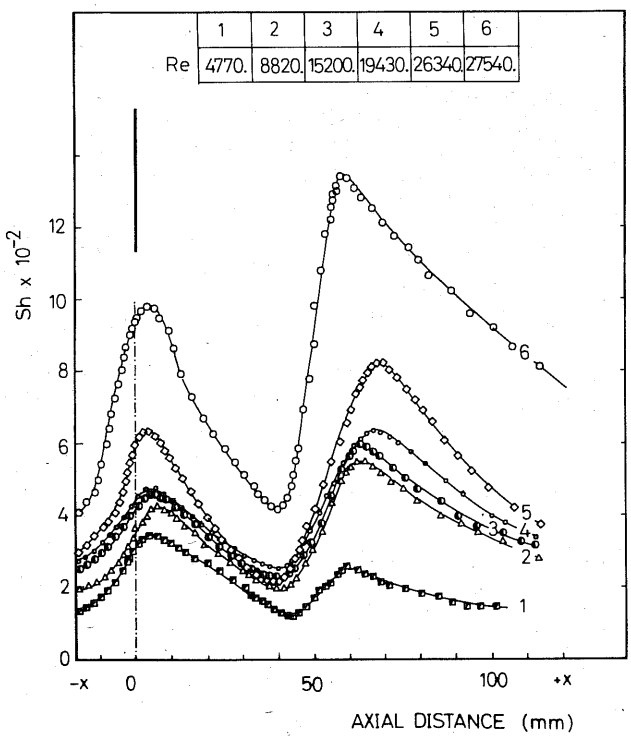

Fig. 5. Local Sherwood number vs. tube wall length. Coaxially disk of 2/3 *d*.

constant value of Sherwood number, characteristic for the undisturbed flow through an empty tube at that Reynolds number. In addition, one immediately observes two maxima and one minimum, where the first maximum is lower than the second one. The sudden rise of the curves between the minimum and second maximum is also characteristic.

The first maximum is due to two effects. An increase of the velocity gradient in the axial direction results from the

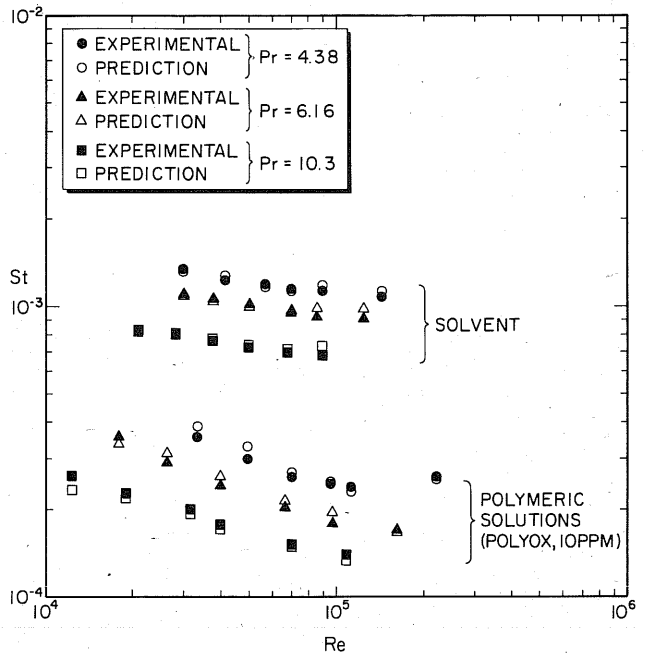

Fig. 1. Comparison of predicted values of Stanton number with experimental data of Debrule (1972).

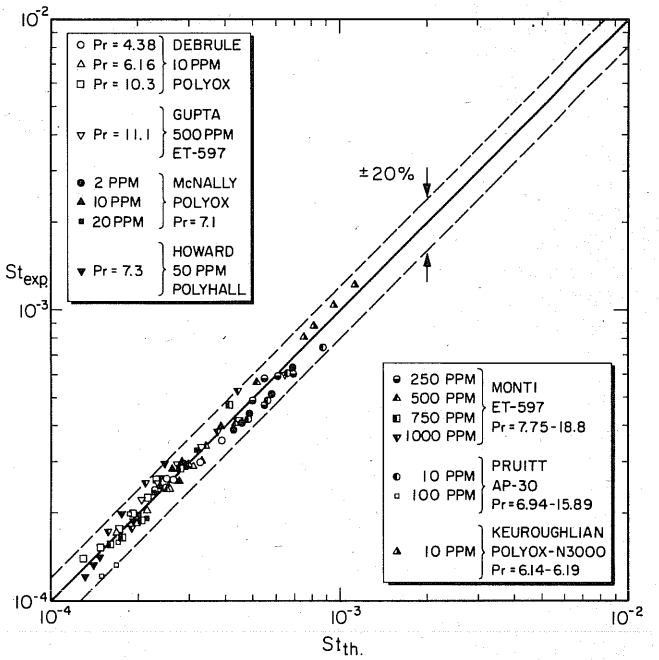

Fig. 2. Comparison of the predicted Stanton number using the present model with measurements.

$$[1 + 2(r/r_o)^2]^2\left[1 - \exp\left(\frac{-(1 - r/r_o)}{A^+/r_o{}^+}\right)\right]^2\Bigg\}^{1/2} - \frac{1}{2} \tag{1}$$

From this expression, the time-average momentum equation can be integrated to yield the mean velocity profile

$$\overline{U}(\overline{r}) = \frac{Ref}{4}\int_{\overline{1}}^{\overline{r}} \frac{r_1}{1 + E(r_1)}\, dr_1 \tag{2}$$

A second integration yields the mass average velocity

$$U_m = \frac{2}{r_o{}^2}\int_o^{r_o} U\, r\, dr \tag{3}$$

The nondimensional form of Equation (3)

$$1 = \frac{Ref}{2}\int_o^1\int_1^{\overline{r}} [r_1/(1 + E(r_1))\, dr_1]\, \overline{r}\, d\overline{r} \tag{4}$$

is used to determine the final and appropriate value of A^+ because the precise form of Equation (1) must be such that Equation (4) is valid for the experimental inputs of Re and f. This differs from the normal Newtonian flow procedure where A^+ is specified as an input. In drag reducing flows this is not appropriate because the thickness of the wall region increases, and it is not possible to determine A^+ a priori. It is possible to specify the von Karman constant K because it has been established (see Virk, 1975) that the slope in the logarithmic portion of the velocity profile is the same as the slope in a Newtonian flow.

With the velocity profile known and with the Reynolds analogy assumption that $\epsilon_H = \epsilon_M$, integration of the energy equation is straightforward. The heat transfer coefficient is defined by

$$\dot{q}_o'' = h(T_o - T_m) \tag{5}$$

where

$$\dot{q}_o'' = k(\partial T/\partial r)_{r=r_o} \tag{6}$$

Therefore, the temperature profile obtained from the energy equation is used to evaluate h and the Stanton number. For a constant heat flux at the wall, the equation for the Stanton number becomes

$$St = \frac{\displaystyle\int_1^o \overline{U}\,(1 - \overline{y})\, d\overline{y}}{Re\displaystyle\int_o^1 \overline{U}(1 - \overline{y})\left\{\int_o^{\overline{y}}\left[\frac{\displaystyle\int_1^{\overline{y}_1}\overline{U}(1 - \overline{y}_2)\, d\overline{y}_2}{\left(\dfrac{\epsilon_H}{\nu} + \dfrac{1}{Pr}\right)(1 - \overline{y}_1)}\right] d\overline{y}_1\right\} d\overline{y}} \tag{7}$$

Consequently, estimates of two additional physical properties of the drag reducing solution (the thermal conductivity k and the Prandtl number Pr) are needed to predict the heat transfer coefficient. When these properties of the solution are known, there is no difficulty. However, typically, these properties are not known, and estimates must be made. In this study, when the concentration of the solution was less than 50 p.p.m., the values of k and Pr were assumed to be the same as those of water at the temperature of the solution. For the concentrated solutions, the thermal conductivity of the solution was taken to be that of pure water, and the Prandtl number was obtained from

the viscosity of the concentrated solution and the thermal conductivity estimate.

The heat transfer prediction scheme for the drag reducing fluids outlined in this brief was compared with the prediction techniques of Poreh and Paz (1968), Wells (1968), Smith et al. (1969), and the results of the seven drag reducing heat transfer experiments of Debrule (1972), Howard (1971), Pruitt et al. (1966), Keuroughlian (1967), Gupta et al. (1967), McNally (1968), and Monti (1972). These experiments provided enough information to start the calculations and used different types of polymer at different concentrations. The Reynolds and Prandtl numbers in these experiments ranged from 5.5×10^3 to 2.5×10^5 and 4.4 to 18.8, respectively (see Ghajar, 1975).

The point-by-point comparison of the predicted values of Stanton numbers with the experimental data of Debrule (1972) for 10 p.p.m. WSR-301 Polyox solution at three different Prandtl numbers are shown in Figure 1. The agreement with experimental results is considered to be very good. The solvent data are also shown on the same figure to demonstrate the amount of reduction in heat transfer $[(St_{water} - St_{poly})/St_{water}]$.

Figure 2 compares the theoretical values of Stanton numbers calculated from the measured values of the friction factor, Prandtl, and Reynolds number of seven drag reducing heat transfer experiments using the present theoretical model with the experimental values. The agreement between the theoretical and experimental values is very reasonable. Almost all of the experimental data are predicted within $\pm$ 20% by the model. A similar comparison was made for solvent experimental data, and all of the predictions were within $\pm$ 10% of the experimental data.

Some of the experimental data of Howard (1971), Pruitt et al. (1966), and Keuroughlian (1967) shown in Figure 2 were not predicted very well by the present model with $K = 0.4$. The problem was investigated, and it was found that the friction factors corresponding to those particular data all fall on or above the maximum drag reduction asymptote as given by Virk (1971). For those data points, the value of K, the von Karman constant, was changed from a value of 0.4 to 1/11.7 since, according to Virk, for the case of maximum drag reduction the fully turbulent logarithmic region does not exist and the value of K should correspond to the slope of the elastic sublayer region. This change in K improved the predicted values. In addition, this change renders the previous interpretation of A^+ invalid because when the elastic sublayer extends all the way to the center line, A^+ cannot characterize the thickness of the wall layer.

The sensitivity of the present model was checked against the variation in the Prandtl number and friction factor measurements. These two parameters were chosen because they have a direct effect on the heat transfer predictions. A probable error of $\pm$ 10% was considered for the reported values of Pr and f. Three different sets of experimental data were used to demonstrate the independent effect of these variations upon the predictions. The calculations show that the present model is relatively insensitive to Prandtl number errors and somewhat more sensitive to the accuracy of the pressure drop measurements (see Ghajar, 1975).

From experimental data, the suggested model of this study was compared with the theoretical models of Poreh and Paz (1968) and Wells (1968) and correlation of Smith et al. (1969). For most drag reducing flows, the model predicted the experimental heat transfer rates as well or better than these other prediction techniques (see Ghajar, 1975). The correlation of Smith et al. (1969) yields somewhat better estimates of h for flows in which the friction factor is on the maximum drag reduction asymptote. However, this correlation is not as general as the suggested model of this study because the correlation is based solely upon the heat transfer experiments of Keuroughlian (1967), where the condition of maximum drag reduction was achieved in each flow.

The present model is simple, inexpensive, requires a relatively small amount of information, and does a good job of predicting the velocity profile, eddy diffusivity distribution, and temperature profile, as well as the heat transfer coefficient.

NOTATION

A^+ = constant that characterizes thickness of wall layer in Van Driest's law
E = nondimensional eddy diffusivity, ϵ/ν
f = Fanning friction factor, $f = 2\tau_w/\rho U_m^2$
h = heat transfer coefficient
k = thermal conductivity
K = von Karman constant
Pr = Prandtl number
q_o'' = heat transfer rate per unit area at the tube surface
Re = Reynolds number, $Re = (2r_o) U_m/\nu$
r = radial coordinate
$\bar{r}$ = nondimensional radial coordinate, $\bar{r} = r/r_o$
r_o = radius of pipe
r_o^+ = nondimensional pipe radius, $r_o^+ = r_o U_\tau/\nu$
St = Stanton number
T = mean temperature
T_m = mixed mean temperature
T_o = fluid temperature at surface
U = streamwise mean velocity
$\bar{U}$ = nondimensional streamwise mean velocity, $\bar{U} = U/U_m$
U_m = mass average velocity
U_τ = shear velocity, $U_\tau = (\tau_w/\rho)^{1/2}$
$\bar{y}$ = nondimensional direction normal to wall, $\bar{y} = y/r_o$
y = coordinate direction normal to wall

GREEK LETTERS

ν = kinematic viscosity
ρ = fluid density
ϵ_H = eddy diffusivity for heat
ϵ_M = eddy diffusivity for momentum
τ_w = wall shear stress

LITERATURE CITED

Cess, R. D., "A Survey of the Literature in Heat Transfer in Turbulent Tube Flow," *Westinghouse Res. Rept. 8-0529-R24*, Westinghouse Corporation, Philadelphia, Pa. (1958).

Debrule, P. M., "Friction and Heat Transfer Coefficient in Smooth and Rough Pipes with Dilute Non-Newtonian Fluids in Pipes," Ph.D. theses, Calif. Inst. Technol. (1972).

Ghajar, A. J., "Prediction of Heat Transfer Coefficients in Drag Reducing Turbulent Pipe Flows," M.S. thesis, Okla. State Univ., Stillwater (1975).

Gupta, M. K., A. B. Metzner, and J. P. Hartnett, "Turbulent Heat Transfer Characteristics of Viscoelastic Fluids," *Intern. J. Heat Mass Transfer*, **10**, 1211 (1967).

Howard, R. G., "Characterization of Heat and Momentum Transfer for Polyox WSR-301 and Polyhall M-295 Solutions," *Rept. No. 7-551*, Naval Ship Research and Development Center, Washington, D. C. (1971).

Keuroughlian, G. H., "Heat Transfer to Dilute Polymer Solutions," M. S. thesis, Mass. Inst. Technol., Cambridge (1967).

McNally, W. A., "Heat and Momentum Transport in Dilute Polyethylene Oxide Solutions," Ph.D. thesis, Univ. Rhode Island (1968).

Monti, R., "Heat Transfer in Drag Reducing Solution," in *Progresses in Heat Transfer*, Vol. 5, pp. 239-261, Pergamon Press, Oxford, England (1972).

Poreh, M., and U. Paz, "Turbulent Heat Transfer to Dilute Polymer Solutions," *Intern. J. Heat Mass Transfer*, **11**, 805 (1968).
Pruitt, G. T., N. F. Whitsitt, and H. R. Crawford, "Turbulent Heat Transfer to Viscoelastic Fluids," *Rept. No. NAS7-369* Western Company, Dallas, Tex. (1966).
Smith, K. A., G. H. Keuroughlian, P. S. Virk, and E. W. Merrill, "Heat Transfer to Drag Reducing Polymer Solutions," *AICHE J.*, **15**, 294 (1969).
Tiederman, W. G., and M. M. Reischman, "Calculation of Velocity Profiles In Drag-Reducing Flow," *Trans. ASME, J. Fluids Eng.* (1976).
Virk, P. S., "An Elastic Sublayer Model for Drag Reduction by Dilute Polymer Solutions of Linear Macromolecules," *J. Fluid Mech.*, **45**, 417 (1971).
———, "Drag Reduction Fundamentals," *AICHE J.*, **21**, 625 (1975).
Wells, C. S., "Turbulent Heat Transfer in Drag Reducing Fluids," *ibid.*, **14**, 406 (1968).

Manuscript received July 6, 1976; revision received November 2, and accepted November 8, 1976.

Immiscible Liquid Displacement In A Capillary Tube: The Moving Contact Line

E. B. DUSSAN V.

Department of Chemical and Biochemical Engineering
University of Pennsylvania
Philadelphia, Pennsylvania 19174

The internal deformation of two immiscible liquids as one displaces the other on flowing through a circular capillary tube is examined. The existence of a toroidal-like flow adjacent to the moving interface is documented. These observations may be relevant when liquid-liquid systems are modeled in which a surfactant is present, as in the case of oil recovery. Measurements of this flow may also lead to a better understanding of the moving contact line.

Place a glass capillary tube vertically over a dish of water. The moment the lower end of the tube touches the air-water interface, a column of water (one immiscible fluid) rises up the tube and displaces the air (the other immiscible fluid) until it reaches an equilibrium height. The dynamics of the displacing fluids has been studied over the years with particular emphasis placed on liquid-gas systems. For these systems it has been found that the details of the fluid motion in the region immediately adjacent to the fluid-fluid interface can essentially be ignored when the speed at which the interface travels through the tube is analyzed. [G. D. West (1911-1912) was the first person to successfully model the flow in a capillary tube and predict the speed of propagation of the fluid-fluid interface. He assumed that the fluids undergo Poiseuille flow up to a point about two tube diameters to either side of the fluid-fluid interface. In the region near the interface the only significant pressure drop was assumed to come from its surface tension and curvature. By assuming the curvature of the interface was known, he avoided having to do any detailed analysis in the region. Others who rediscovered this include E. W. Washburn (1921) and G. D. Yarnold (1938).] However, for systems consisting of two immiscible liquids and a soluble surfactant, such simplifying assumptions may no longer be appropriate. The surfactant, in order for it to be effective, must be present at the liquid-liquid interface where it must reduce the interfacial tension to an exceedingly small value. This essentially eliminates the capillary force, whose presence, for example, impedes the movement of small slugs of oil trapped within porous rock. Does the surfactant remain at the liquid-liquid interface, or is it pushed off and forced onto the walls of the solid matrix? Is the surfactant readily accessible to the interface, or is it depleted from the surrounding liquid thus reducing the rate at which additional surfactant can be adsorbed onto the interface? It is evident that the motion of the liquids in the region surrounding the interface is an important factor.

In this note the motion of the fluids in the vicinity of the fluid-fluid interface is examined in detail for a system consisting of two immiscible liquids flowing through a circular capillary tube. It is shown that one fluid undergoes the familiar fountain type of motion, while the other fluid contains a region adjacent to the interface where in a more complicated toroidallike motion occurs. This latter motion has not been previously observed. [In an attempt to explain the experimentally observed fact that the curvature of the interface is constant for slow flow, Rose (1961) postulates a different flow field].

There is a more fundamental reason for studying this system. A contact line moving over a solid surface (for systems consisting of either two immiscible liquids, or a liquid and a gas) occurs in countless natural and industrial processes; however, to this day the dynamics of the moving contact line is not understood. One approach has been

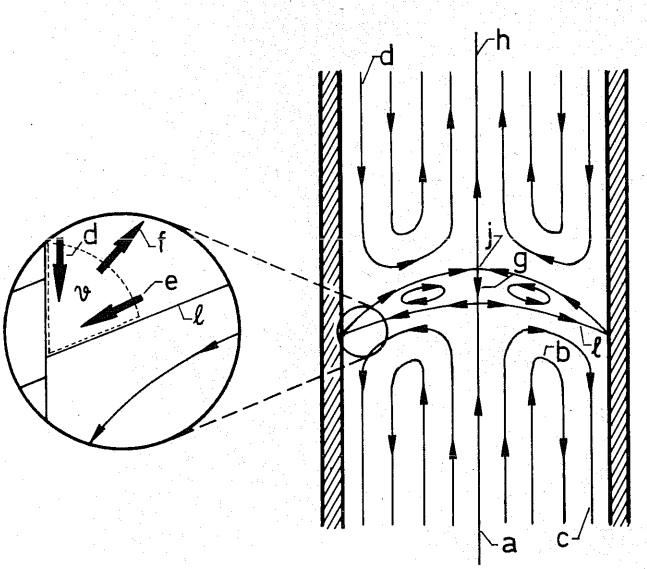

Fig. 1. Conceptualization of flow field.